

BALL PACKINGS FOR LINKS

JORGE L. RAMÍREZ ALFONSÍN AND IVAN RASSKIN

ABSTRACT. The *ball number* of a link L , denoted by $\text{ball}(L)$, is the minimum number of solid balls (not necessarily of the same size) needed to realize a necklace representing L . In this paper, we show that $\text{ball}(L) \leq 5cr(L)$ where $cr(L)$ denotes the *crossing number* of L . To this end, we use Lorentz geometry applied to ball packings. The well-known Koebe-Andreev-Thurston circle packing Theorem is also an important brick for the proof. Our approach yields to an algorithm to construct explicitly the desired necklace representation of L in \mathbb{R}^3 .

1. INTRODUCTION

A *chain of balls* is a sequence of non-overlapping solid balls in the space where all the consecutive balls are tangent. The *thread* of a chain of balls is the polygonal curve formed by joining the centers of consecutive tangent balls with straight segments. A chain of balls is *closed* if the last ball is tangent to the first ball. The thread of a closed chain can be thought of as a polygonal knot in the space. A *necklace representation* of a link L is a collection of non-overlapping chains of balls such that their threads forms a polygonal link isotopic to L .

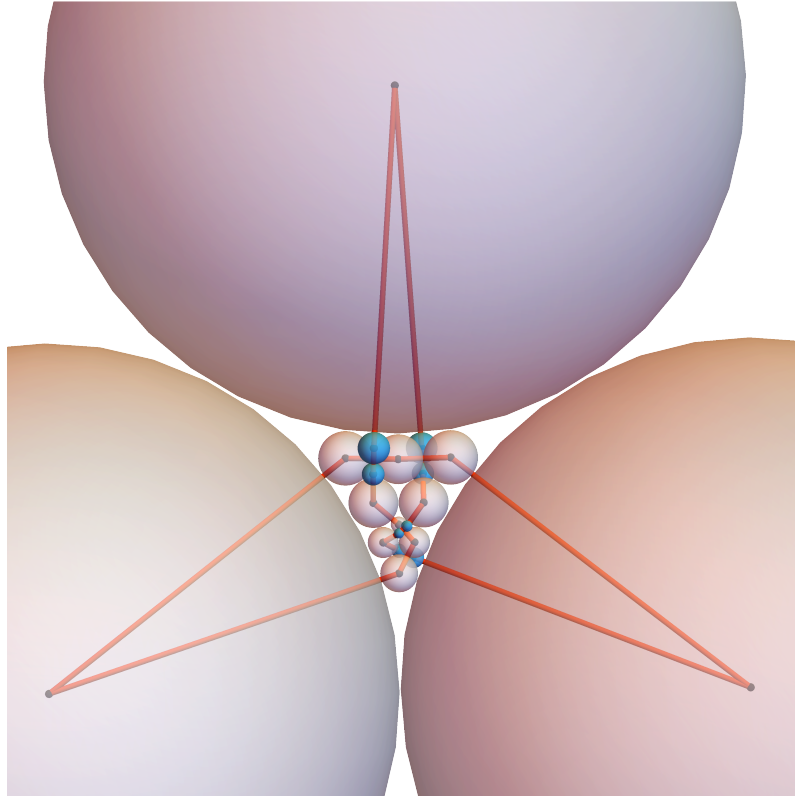


FIGURE 1. A necklace representation of the Figure 8 knot with 20 balls.

In [17], Maehara defined the *ball number* of a link L , denoted by $\text{ball}(L)$, as the minimum number of balls (not necessarily of the same size) needed to construct a necklace representation of L . Little is known about the behavior of $\text{ball}(L)$. Maehara proved that $9 \leq \text{ball}(3_1)$ in [17, Theorem 9]. Some years earlier, Maehara and Oshiro showed that $\text{ball}(3_1) \leq 12$ in [20, Theorem 5] and that $\text{ball}(2_1^2) = 8$ in [19, Theorem 2]. As far as we are aware, these are the only known results concerning ball numbers of links.

2020 *Mathematics Subject Classification.* 52C17, 57K10.

Key words and phrases. Ball packings, Links, Lorentzian space.

Necklace representations can be regarded as a particular case of polygonal representations of links with a strong geometric condition. Polygonal representations of links have been of great interest not only in mathematics but also in chemistry and physics. Indeed, polygonal representations has been applied to the study of the DNA and knotted molecules [11].

In this paper we present the following upper bound to $\text{ball}(L)$.

Theorem 1. *Let L be a link. Then,*

$$\text{ball}(L) \leq 5cr(L)$$

where $cr(L)$ denotes the crossing number of L , that is, the minimal number of crossings in any diagram for L .

Our approach allows to come up with an algorithm to construct explicitly the necklace representing the link L . We are able to compute the coordinates of the centers and the radius of each of the balls of the desired necklace.

Unfortunately, our technique do not allow us to push further the above upper bound. However, we believe that it can be improved.

Conjecture 1. *Let L be a link. Then,*

$$\text{ball}(L) \leq 4cr(L).$$

Moreover, the equality holds if L is alternating.

Given the connection of the ball number with the so-called Koebe-Andreev-Thurston circle packing Theorem (see below) a linear bound seems inevitable.

A close related invariant to the ball number is the *pearl number* of a link L in which the balls have to be of the same size. The latter seems closely connected to another geometric invariant, the *rope length* of L . There is known a quasilinear upper bound on rope length in terms of the crossing number and a linear upper bound is conjectured. In [10], it is given a sequence of knots such that the rope length grows linearly in the crossing number. It is natural to ask whether the latter can be refined to pearl necklaces with unequal pearls.

The paper is self-contained and it is organized as follows. In the next section, we briefly introduce some basic notions on the space of d -balls. We then explain the Lorentzian model for the space of d -balls and its connections with the inversive geometry. We also discuss some definitions and properties of the inverse product and the action of the Möbius group on the space of d -balls.

In Section 3, after recalling classical background of ball packing theory we introduce and study some geometric properties of both *pyramidal disk systems* and *crossing ball systems*. These are two fundamental bricks for our construction.

In Section 4, we prove our main result. Let us give a brief outline of the proof. The strategy runs as follows. Combining the projection of a link and its associated *medial graph* we construct a simple planar graph which contains a subgraph isotopic to the projection of the given link. We then consider a disk packing associated to such planar graph obtained by using the Koebe-Andreev-Thurston circle packing Theorem. The latter able us to construct a ball packing by a *blowing up*. Afterwards, we associate to each crossing a *crossing ball system* (creating the appropriate *bridges* by adding only two extra balls to represent the given link). We finally stick together such systems. We use inversive geometry in order to verify that our construction works properly.

Finally, in Section 5, we will present an algorithm (based on the approach used in the proof of Theorem 1) that outputs the coordinates of the centers and the radius of the balls forming the necklace representation of the given link L . The examples presented in this paper have been done throughout an implementation of this algorithm.

2. THE SPACE OF d -BALLS.

2.1. From spherical caps to d -balls. Some notations and definitions of this section can be found in the PhD thesis of Chen [7] and the paper of Wilker *Inversive geometry* [23]. Let $d \geq 1$ be an integer. We denote \mathbb{R}^d the euclidean space of dimension d and $\langle \cdot, \cdot \rangle_2$, $\| \cdot \|$ the euclidean inner product and the euclidean norm respectively. Let \mathbb{S}^d be the unit d -sphere of \mathbb{R}^{d+1} endowed with the induced metric $\| \cdot \|_{\mathbb{S}}$ from \mathbb{R}^{d+1} . A d -spherical cap α of center $c \in \mathbb{S}^d$ and spherical radius $\rho \in (0, 2\pi)$ is the subset

$$(1) \quad \alpha = \{x \in \mathbb{S}^d \mid \|x - c\|_{\mathbb{S}} \leq \rho\}$$

which gives a partition of \mathbb{S}^d in three disjoint subsets: the *interior* of α , $int(\alpha)$, points of \mathbb{S}^d satisfying (1) strictly, the *exterior* of α , $ext(\alpha)$, points of \mathbb{S}^d not satisfying (1) and the boundary of α , $\partial\alpha$, points of \mathbb{S}^d satisfying the equality of (1). We note $\text{Caps}(\mathbb{S}^d)$ the space of d -spherical caps. It is well known that \mathbb{S}^d is homeomorphic to $\widehat{\mathbb{R}^d}$ under the stereographic projection where $\widehat{\mathbb{R}^d} := \mathbb{R}^d \cup \{\infty\}$ is the one-point compactification of \mathbb{R}^d . A d -ball of $\widehat{\mathbb{R}^d}$ is the image of a d -spherical cap under the stereographic projection. We denote $\text{Balls}(\widehat{\mathbb{R}^d})$ the space of d -balls, isomorphic to $\text{Caps}(\mathbb{S}^d)$ given by the above construction. Moreover, a d -ball b is called *solid ball*, *hollow ball* and *half-space* depending on whether the pole of the stereographic projection lies in the exterior, interior or boundary of the corresponding d -spherical cap α_b , see Figure 4.

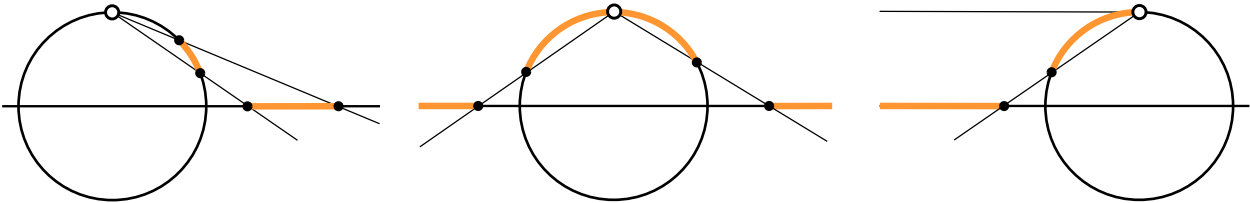


FIGURE 2. Examples of a solid ball, a hollow ball and a half-space.

More precisely, a d -ball of $\widehat{\mathbb{R}^d}$ of curvature $\kappa \in \mathbb{R}$ will be one of the following subsets:

- *Solid ball*: $\{x \in \widehat{\mathbb{R}^d} \mid \|x - c\| \leq \frac{1}{\kappa}\}$ when $\kappa > 0$.

It is also a standard d -ball of \mathbb{R}^d with center $c \in \mathbb{R}^d$ and radius $\frac{1}{\kappa}$.

- *Hollow ball*: $\{x \in \widehat{\mathbb{R}^d} \mid \|x - c\| \geq -\frac{1}{\kappa}\}$ when $\kappa < 0$.

It can be regarded as the union of the exterior of a solid ball with its boundary.

- *Half-space*: $\{x \in \widehat{\mathbb{R}^d} \mid \langle x, n \rangle_2 \leq \delta\}$ when $\kappa = 0$.

By convention, we choose the *normal vector* n which points towards the interior. The real number δ represents the *algebraic distance* from the boundary to the origin (positive if the origin is contained in the interior and negative otherwise).

There is a natural embedding of $\text{Balls}(\widehat{\mathbb{R}^d}) \hookrightarrow \text{Balls}(\widehat{\mathbb{R}^{d+1}})$ where a d -ball b of center c and curvature κ (resp. normal vector n and algebraic distance δ) is mapped to a $(d+1)$ -ball \hat{b} of center $(c, 0)$ and curvature κ (resp. normal vector $(n, 0)$ and algebraic distance δ). We call this mapping the *blowing up*.

2.2. The angle between two d -balls with intersecting boundaries. For $d > 1$, let b and b' two d -balls with intersecting boundaries. We define the *angle between b and b'* , denoted $\angle(b, b') \in [0, \pi]$, as the angle formed by the vectors \vec{pc} and \vec{pc}' where c and c' are the centers of b and b' and $p \in \partial b \cap \partial b'$, see Figure 3. $\angle(b, b')$ does not depend on the choice of the point in the intersection.

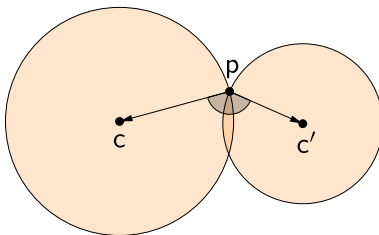


FIGURE 3. The angle between two 2-balls in gray.

Two d -balls b and b' with intersecting boundaries are said to be:

- *Internally tangent* if $\angle(b, b') = 0$.
- *Orthogonal* if $\angle(b, b') = \frac{\pi}{2}$.
- *Externally tangent* if $\angle(b, b') = \pi$.

When the boundaries of b and b' do not intersect the angle $\angle(b, b')$ is not well-defined. In this case we say that b and b' are *disjoint* if they have disjoint interiors and *nested* otherwise. When b and b' are nested there is one of both which is contained in the other.

Remark 1. *The blowing up preserves angles.*

We notice that the previous definition of angle does not work when $d = 1$ since the boundary of a 1-ball is not simply connected. In this case we can define the angle between two intersecting 1-balls b and b' as the angle between the 2-balls \widehat{b} and \widehat{b}' obtained by blowing-up.

2.3. The hyperbolic model for $\text{Balls}(\widehat{\mathbb{R}^d})$. Let \mathbb{H}^{d+1} be the Poincaré ball model of the hyperbolic space of dimension $d + 1$ embedded in $\widehat{\mathbb{R}^{d+1}}$ as the standard unit $(d + 1)$ -ball. The boundary $\partial\mathbb{H}^{d+1}$ is exactly the unit sphere \mathbb{S}^d . A d -hyperbolic half-space of \mathbb{H}^{d+1} is the intersection $h := \mathbb{H}^{d+1} \cap \widehat{b}_h$ where \widehat{b}_h is a $(d + 1)$ -ball orthogonal to \mathbb{H}^{d+1} . We denote $\text{Halfs}(\mathbb{H}^{d+1})$ the space of hyperbolic half-spaces of \mathbb{H}^{d+1} . At the boundary of \mathbb{H}^{d+1} , the intersection $\partial\mathbb{H}^{d+1} \cap \widehat{b}_h = \mathbb{S}^d \cap \widehat{b}_h$ is a d -spherical cap α_h which corresponds to a d -ball b_h by the stereographic projection. For any d -ball, the mapping $h \mapsto \alpha_h \mapsto b_h$ can be easily reversed so we have the bijections

$$(2) \quad \text{Halfs}(\mathbb{H}^{d+1}) \longleftrightarrow \text{Caps}(\mathbb{S}^d) \longleftrightarrow \text{Balls}(\widehat{\mathbb{R}^d})$$

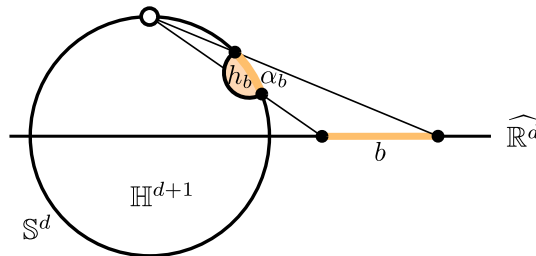


FIGURE 4. A d -ball and its corresponding hyperbolic half-space.

The notions of interior, exterior and boundary are easily extended for d -hyperbolic half-spaces. For $d > 1$, two d -balls b have intersecting boundaries if and only if the corresponding d -hyperbolic half-spaces h_b and $h_{b'}$ have intersecting boundaries. Moreover, $\angle(b, b')$ is equal to the *dihedral angle* of h_b and $h_{b'}$ measured at a *non-common region*.

2.4. The Lorentzian model for $\text{Balls}(\widehat{\mathbb{R}^d})$. The Lorentzian space of dimension $d + 2$, denoted by $\mathbb{L}^{d+1,1}$, is a real vector space of dimension $d + 2$ equipped with a bilinear symmetric form $\langle \cdot, \cdot \rangle$ of signature $(d + 1, 1)$. The *Lorentzian product* of two vectors u and v of $\mathbb{L}^{d+1,1}$ is the real number $\langle u, v \rangle$ and the *Gramian* of a collection of vectors $\mathcal{V} = \{v_1, \dots, v_n\}$ of $\mathbb{L}^{d+1,1}$ is the matrix

$$\text{Gram}(\mathcal{V}) := \begin{pmatrix} \langle v_1, v_1 \rangle & \cdots & \langle v_1, v_n \rangle \\ \vdots & \ddots & \vdots \\ \langle v_n, v_1 \rangle & \cdots & \langle v_n, v_n \rangle \end{pmatrix}$$

If $\mathcal{V} = \{v_1, \dots, v_{d+2}\}$ is a basis of $\mathbb{L}^{d+1,1}$ then the $\text{Gram}(\mathcal{V})$ is the matrix of the Lorentzian product in the basis \mathcal{V} which means that the Lorentzian product of two vectors $u, v \in \mathbb{L}^{d+1,1}$ can be computed by

$$(3) \quad \langle u, v \rangle = C_{\mathcal{V}}(u)^T \text{Gram}(\mathcal{V}) C_{\mathcal{V}}(v)$$

where $C_{\mathcal{V}}(\cdot)$ denotes the column-matrix of the Cartesian coordinates respect to \mathcal{V} . Generalizing the definition of Boyd in [4], we define the *polyspherical coordinates* of a vector $u \in \mathbb{L}^{d+1,1}$ respect to \mathcal{V} as the column-matrix $P_{\mathcal{V}}(u) = (\langle v_1, u \rangle \cdots \langle v_{d+2}, u \rangle)^T$ which is related to the Cartesian coordinates by

$$(4) \quad C_{\mathcal{V}}(u) = \text{Gram}(\mathcal{V})^{-1} P_{\mathcal{V}}(u)$$

Combining equations (3) and (4) we can compute the Lorentzian product in polyspherical coordinates by

$$(5) \quad \langle u, v \rangle = P_{\mathcal{V}}(u)^T \text{Gram}(\mathcal{V})^{-1} P_{\mathcal{V}}(v)$$

In the practice we will use equation (5) to compute the Lorentzian product in different basis.

In [23], Wilker defined the *inversive coordinates*, $i(b)$, of a d -ball b as the column-matrix of the Cartesian coordinates of v_b respect to \mathcal{V}_0 . These coordinates can be given in terms of the curvature and center (normal vector and algebraic distance for half-spaces) by

$$(8) \quad i(b) = \begin{cases} \frac{\kappa}{2}(2c, \|c\|^2 - \frac{1}{\kappa^2} - 1, \|c\|^2 - \frac{1}{\kappa^2} + 1)^T & \text{if } \kappa \neq 0 \\ (\mathbf{n}, \delta, \delta)^T & \text{if } \kappa = 0 \end{cases}$$

With the inversive coordinates one can compute the inversive product by

$$(9) \quad \langle b, b' \rangle = i(b)^T Q i(b')$$

where $Q = \text{diag}(1, \dots, 1, -1)$ is the Gramian of \mathcal{V}_0 .

2.5. The Möbius group. A *Lorentz transformation* is a linear transformation of $\mathbb{L}^{d+1,1}$ which preserves the Lorentzian product and the *Lorentz group*, $O(d+1,1)$, is the group of all the Lorentz transformations. The *Orthochronous Lorentz group* is the subgroup $O^\uparrow(d+1,1) < O(d+1,1)$ of all the Lorentz transformations preserving the time direction. The generators of $O^\uparrow(d+1,1)$ are the *Lorentzian reflections* on the boundary of time-like half-spaces t_v

$$(10) \quad \sigma_v : u \mapsto u - 2\langle u, v \rangle v$$

with $v \in S(\mathbb{L}^{d+1,1})$. We notice that $\sigma_v(v) = -v$, $\sigma_v = \sigma_{-v}$ and $\sigma_v(u) = u$ if and only if $\langle u, v \rangle = 0$. The Orthochronous Lorentz group acts on $S(\mathbb{L}^{d+1,1})$. Composing with the isomorphisms of (6) one gets the following commutative diagram

$$(11) \quad \begin{array}{ccccccc} O^\uparrow(d+1,1) & \longleftrightarrow & Isom(\mathbb{H}^{d+1}) & \longleftrightarrow & Aut(\mathbb{S}^d) & \longleftrightarrow & Möb(d) \\ \downarrow & & \downarrow & & \downarrow & & \downarrow \\ S(\mathbb{L}^{d+1,1}) & \longleftrightarrow & Halfs(\mathbb{H}^{d+1}) & \longleftrightarrow & Caps(\mathbb{S}^d) & \longleftrightarrow & Balls(\widehat{\mathbb{R}}^d) \end{array}$$

where $Isom(\mathbb{H}^{d+1})$ is the group of isometries of \mathbb{H}^{d+1} , $Aut(\mathbb{S}^d)$ is the group of conformal automorphisms of \mathbb{S}^d and $Möb(d)$ is the *Möbius Group* which can be defined as the group of the continuous automorphisms of $\widehat{\mathbb{R}}^d$ mapping d -balls to d -balls [22] (some authors make no difference between the last two groups [21]). An element of the Möbius Group is called a *Möbius transformation*. An *inversion in a d -ball b* can be defined as the only Möbius transformation which maps b to $-b$ and fixes a d -ball b' if and only if b' is orthogonal to b [22]. The isomorphisms of (11) map an inversion in a d -ball b into a Lorentzian reflection on the boundary of a time-like half-space t_{v_b} and therefore the Möbius Group is generated by inversions. We denote σ_b the inversion in the d -ball b . When b has zero curvature σ_b is a reflection on the boundary of b which is an hyperplane of \mathbb{R}^d . In addition, the product of two inversions in d -balls centered at the origin with non-zero curvatures κ and κ' gives a *dilatation* of \mathbb{R}^d of ratio $(\kappa'/\kappa)^2$. Thus, the group of isometries and dilatations of \mathbb{R}^d is a subgroup of $Möb(d)$.

3. d -BALL PACKINGS

A collection of d -balls $\mathcal{P} = \{b_1, \dots, b_n\}$ in $\widehat{\mathbb{R}^d}$ is called a d -ball packing if every pair of d -balls $b_i, b_j \in \mathcal{P}$ are either externally tangent or disjoint. The *tangency graph* of a d -ball packing \mathcal{P} is the simple graph $G = (V, E)$ where $V = \{1, \dots, n\}$ and $E = \{ij \mid b_i \text{ and } b_j \text{ are externally tangent}\}$. A simple graph G is said to be d -ball packable if there is a d -ball packing \mathcal{P}_G with tangency graph G . In this case G can be embedded in $\widehat{\mathbb{R}^d}$ by taking the centers of the d -balls of \mathcal{P}_G and the straight segments between the centers of any tangent pair. This embedding is usually called the *carrier* of the d -ball-packing, see Figure 6. The Möbius Group preserves inversive products and tangency graphs of d -ball packings. Moreover, Möbius transformations maps carriers to carriers [21].

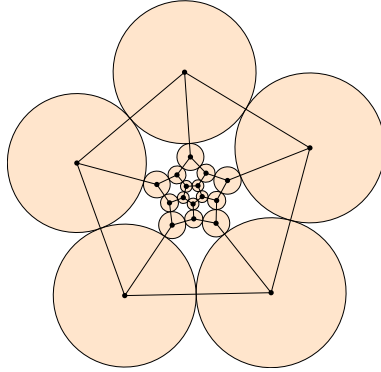


FIGURE 6. A 2-ball packing with its carrier.

A d -ball packing \mathcal{P} is said to be *standard* if it contains the half-spaces $b_i = \{x_d \leq -1\}$ and $b_j = \{x_d \geq 1\}$ and we denote this property by $\mathcal{S}_j^i \mathcal{P}$. The tangency point $b_i \cap b_j$ is at the infinity and the rest of the d -balls of $\mathcal{S}_j^i \mathcal{P}$ must lie inside the region $\{-1 \leq x_d \leq 1\}$. For an edge ij of the tangency graph of \mathcal{P} a *standard transformation* is a Möbius transformation $\phi : \mathcal{P} \mapsto \mathcal{S}_j^i \mathcal{P}$. Such a Möbius transformation exists for every edge ij of G and it can be obtained as the product of an inversion in a d -ball centered at the tangency point $b_i \cap b_j$, an Euclidean isometry and a dilatation of \mathbb{R}^d , see Figure 7.

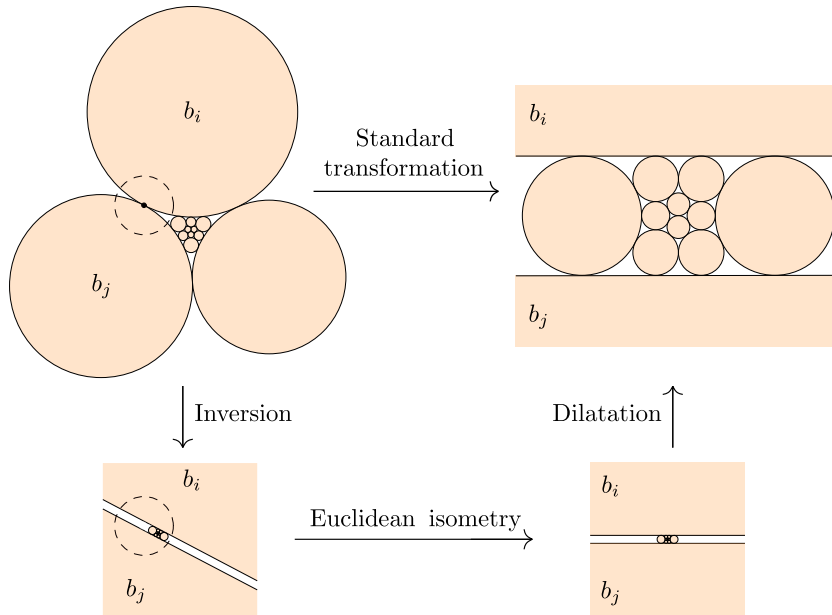


FIGURE 7. Example of a standard transformation.

Two d -ball packings \mathcal{P} and \mathcal{P}' will be said to be *Möbius congruent* if there exists $\mu \in \text{Möb}(d)$ such that $\mu : \mathcal{P} \mapsto \mathcal{P}'$. If in addition μ is an Euclidean isometry then we will say that \mathcal{P} and \mathcal{P}' are *Euclidean congruent*.

Remark 2. Any d -ball packing is Möbius congruent to a d -ball packing formed by solid balls.

For any simple graph G we define the space of equivalence classes under the action of the Möbius Group

$$\mathcal{M}^d(G) := \{d\text{-ball packings with tangency graph } G\} / \text{Möb}(d)$$

We notice that a graph G is d -ball packable if and only if $\mathcal{M}^d(G)$ is not empty. We say that a d -ball packable graph is *Möbius rigid* if all the d -ball packings with tangency graph G are Möbius congruent, which is equivalent to say that $\mathcal{M}^d(G) \simeq 1$. The advantage of a Möbius rigid graph G is that all the properties which are preserved under the action of the Möbius group can be read in just one example of a disk packing \mathcal{P}_G . An useful result to compute the space $\mathcal{M}^d(G)$ is the following:

Lemma 1. *Let \mathcal{P}_G and \mathcal{P}'_G be two d -ball packings with same tangency graph G and let ij be an edge of G . Then \mathcal{P}_G and \mathcal{P}'_G are Möbius congruent if and only if $\mathcal{S}_j^i \mathcal{P}_G$ and $\mathcal{S}_j^i \mathcal{P}'_G$ are Euclidean congruent.*

Proof. Let $\phi : \mathcal{P}_G \mapsto \mathcal{S}_j^i \mathcal{P}_G$ and $\psi : \mathcal{P}'_G \mapsto \mathcal{S}_j^i \mathcal{P}'_G$ be two standard transformations.

(Sufficiency) If $\mathcal{S}_j^i \mathcal{P}_G$ and $\mathcal{S}_j^i \mathcal{P}'_G$ are Euclidean congruent then there is an Euclidean isometry $\gamma : \mathcal{S}_j^i \mathcal{P}_G \mapsto \mathcal{S}_j^i \mathcal{P}'_G$. Then $\psi^{-1} \circ \gamma \circ \phi$ is a Möbius transformation mapping \mathcal{P}_G to \mathcal{P}'_G .

(Necessity) Let us suppose that there is a Möbius transformation $\mu : \mathcal{P}_G \mapsto \mathcal{P}'_G$. Then $\theta := \psi \circ \mu \circ \phi^{-1}$ is a Möbius transformation mapping $\mathcal{S}_j^i \mathcal{P}_G$ to $\mathcal{S}_j^i \mathcal{P}'_G$ and leaving fixed the half-spaces b_i and b_j . Therefore, θ is generated by inversions in d -balls which are simultaneously orthogonal to b_i and b_j . A d -ball simultaneously orthogonal to two parallel half-spaces must be also a half-space. Therefore, θ can be expressed as a product of Euclidean reflections so θ is an Euclidean isometry. \square

The family of d -ball packable graphs are fully characterized for $d = 1, 2$. Such characterization is still unknown nowadays when $d \geq 3$, even for balls. Indeed, it has been proved that recognition of tangency graph is NP-hard for $d = 2, 3, 4$, see [1] and [13]. However, many properties and constructions of 3-ball packable graphs has been found, see [18], [17], [20], [15], [8], [2].

From now on, we shall focus our attention to d -ball packings for $d = 2, 3$. In order to simplify the notation, we will call *disks* (resp. *balls*) the 2-balls (resp. 3-balls) and the collections of disks and balls will be denoted by \mathcal{D} and \mathcal{B} respectively.

Disk packable graph were fully characterized in 1936 by Koebe [14]. The latter was rediscovered by Thurston by using some results of Andreev on hyperbolic 3-polytopes. The well-known Koebe-Andreev-Thurston circle packing Theorem (KAT Theorem) states

Theorem 2. *A graph G is disk packable if and only if G is a simple planar graph. Moreover, if G is a triangulation of \mathbb{S}^2 then G is Möbius rigid.*

For a detailed survey on the applications of the KAT theorem we refer the readers to a recent paper of Bowers [3].

3.1. Pyramidal disk systems. The graph of a polyhedron is the graph made by its vertices and edges. Steinitz proved that the graphs of polyhedra are the 3-connected simple planar graphs. We denote \triangle , \diamond and \boxtimes the graphs of the tetrahedron, octahedron and a square pyramid respectively with the labeling given in Figure 8.

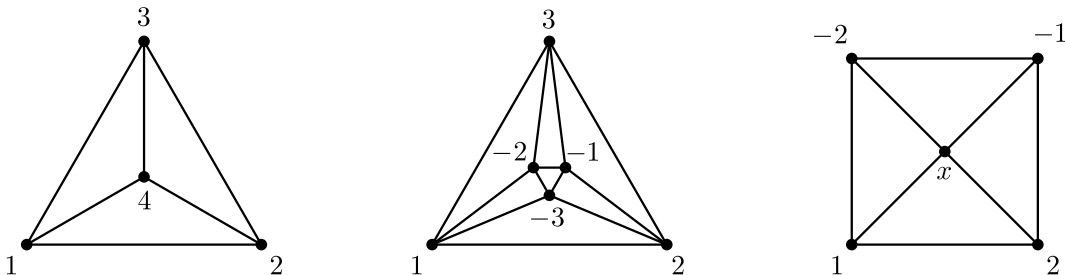


FIGURE 8. Planar embeddings of the graphs \triangle , \diamond and \boxtimes .

Notice that \boxtimes is isomorphic to the subgraph of \diamond obtained by deleting one vertex. These three graphs are simple and planar and hence disk packable by the KAT theorem. We call a disk packing \mathcal{D}_G *tetrahedral*, *octahedral* and *pyramidal* if $G = \triangle$, \diamond , \boxtimes respectively.

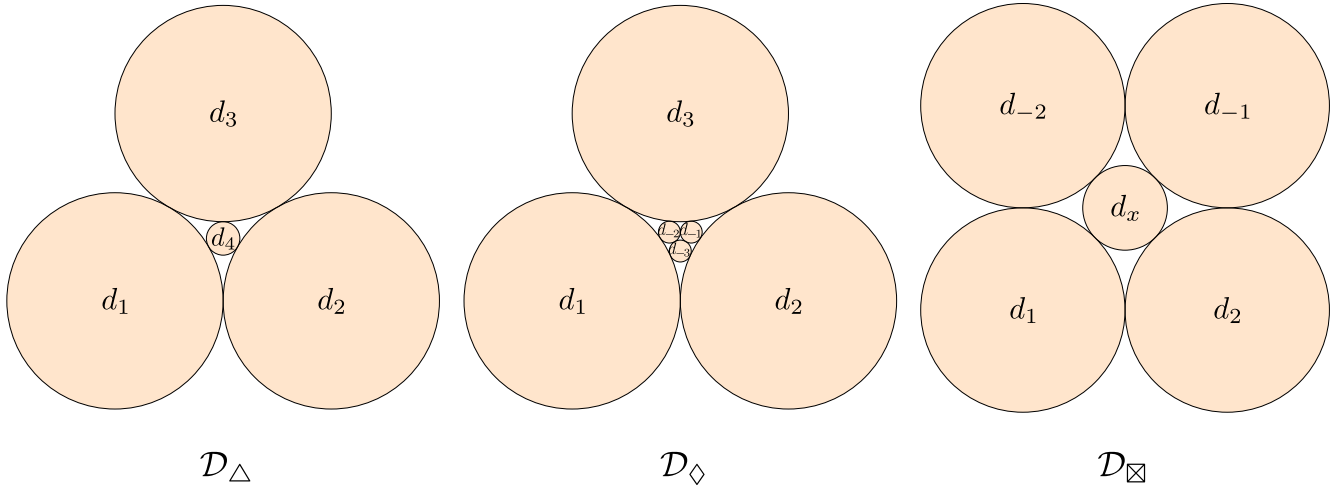


FIGURE 9. A tetrahedral, octahedral and pyramidal disk packings.

Tetrahedral and octahedral disk packings have been well-studied. Since \triangle and \diamond are triangulations of \mathbb{S}^2 , \triangle and \diamond are Möbius rigid. Many nice properties about the behaviour of the curvatures of the disks in tetrahedral and octahedral disk packings can be deduced from the Möbius rigidity, see [16]. Unfortunately, pyramidal disk packings are not Möbius rigid as we show in the following.

Proposition 3.1. $\mathcal{M}^2(\boxtimes) \simeq \mathbb{R}$.

Proof. Let $\mathcal{S}_x^{-1} \mathcal{D}_{\boxtimes}[\kappa_1] = \{d_x, d_1, d_2, d_{-1}, d_{-2}\}$ be a standard disk packing where d_2 and d_{-2} are two unit disks tangent to the half-spaces $d_{-1} = \{y \geq 1\}$, $d_x = \{y \leq -1\}$ and d_1 is a disk of curvature $\kappa_1 \in \mathbb{R}$ tangent to d_2 , d_{-2} and d_x .

First of all, notice that $1 < \kappa_1 < 4$. Indeed, when $\kappa_1 < 1$ (resp. $\kappa_1 > 4$) the disks d_1 and d_{-1} (resp. d_2 and d_{-2}) intersect internally and when $\kappa_1 = 1$ (resp. 4) d_1 and d_{-1} (resp. d_2 and d_{-2}) would be tangent and the tangency graph would be other than \boxtimes , see Figure 10. We also notice that the collection of disk-packings $\{\mathcal{S}_x^{-1} \mathcal{D}_{\boxtimes}[\kappa_1]\}_{1 < \kappa_1 < 4}$ are Euclidean non-congruent. Therefore, by Lemma 1, they represent different equivalence classes in $\mathcal{M}^2(\boxtimes)$. Moreover, these are the only possible standard pyramidal disk packings. Hence, $\mathcal{M}^2(\boxtimes)$ is in bijection to the open interval $(1, 4)$ which is homeomorphic to \mathbb{R} . \square

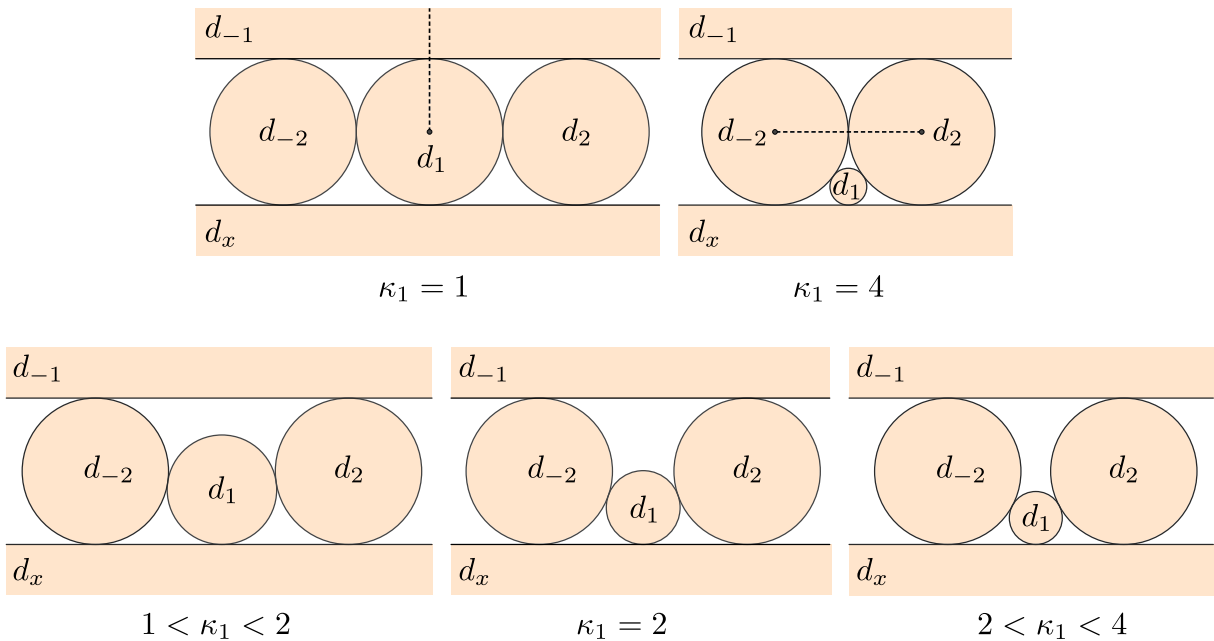


FIGURE 10. Extreme cases with the extra edge (top figures) and the equivalence classes of $\mathcal{M}^2(\boxtimes)$ (below figures).

Pyramidal disk packings are one of the main ingredients for constructing the desire necklace. Since \boxtimes is not Möbius rigid all the properties and the added structures must be carefully verified in each equivalence class of $\mathcal{M}^2(\boxtimes)$. To this end, in the same flavour as in the above proof, we define for every $i = 1, 2 - 1, -2$, the *standard curvatures* of a pyramidal disk packing \mathcal{D}_{\boxtimes} the numbers $1 < \kappa_i < 4$ corresponding to the curvature of the disk d_i in $\mathcal{S}_x^{-i} \mathcal{D}_{\boxtimes}$. The standard curvatures can be used to identify the equivalence class of \mathcal{D}_{\boxtimes} in $\mathcal{M}^2(\boxtimes)$. We define also the *minimal standard curvature* $\kappa := \min\{\kappa_1, \kappa_2, \kappa_{-1}, \kappa_{-2}\}$. We notice that a pyramidal disk packing is a subset of an octahedral disk packing if and only if $\kappa = \kappa_1 = \kappa_2 = \kappa_{-1} = \kappa_{-2} = 2$.

We define a *pyramidal disk system* the collection of disks $(\mathcal{D}_{\boxtimes}, \mathcal{D}_{\boxtimes}^*, d_t)$ formed by

- $\mathcal{D}_{\boxtimes} = \{d_x, d_1, d_2, d_{-1}, d_{-2}\}$: a disk-packing with tangency graph \boxtimes .
- The *mirror disks* $\mathcal{D}_{\boxtimes}^* = \{d_1^*, d_2^*\}$ where d_1^* is the disk orthogonal to d_2, d_{-2}, d_x and d_1 is contained at the interior of d_1^* and d_2^* is the disk orthogonal to d_1, d_{-1}, d_x and d_2 at the interior of d_2^* .
- The *tangency disk* d_t : the disk which its boundary passes through all the tangency points $d_1 \cap d_2, d_1 \cap d_{-2}, d_{-1} \cap d_2$ and $d_{-1} \cap d_{-2}$ and d_x is contained at the interior of d_t .

- The orthogonality conditions of d_1^* imply that the boundary of d_1^* must be the circle with center $(0, -1)$ which passes through the tangency point $d_x \cap d_2$. By simple calculations we have that if the radius of d_1 is $1/\kappa_1$ then the radius of the boundary of d_1^* is $2/\sqrt{\kappa_1}$. The orientation for the interior is determined by the condition $d_1 \subset d_1^*$.

- For d_2^* , a disk orthogonal to d_1 and d_x must be a half-space with boundary the y -axis. As before, the orientation for the interior comes from the condition $d_2 \subset d_2^*$ which gives that d_2^* is the half-space $\{x \geq 0\}$.

- Finally for d_t , by symmetry, the only circle passing through the tangency points $d_1 \cap d_2, d_1 \cap d_{-2}$ and $d_{-1} \cap d_2$ must pass through $d_{-1} \cap d_{-2}$. Again, the orientation is determined from the condition $d_x \subset d_t$.

Since all the conditions which define the mirror disks and the tangency disks are preserved under Möbius transformations, the fact that every disk-packing \mathcal{D}_{\boxtimes} is Möbius congruent to a standard disk packing $\mathcal{S}_x^{-1} \mathcal{D}_{\boxtimes}$ implies that the mirror disks and the tangency disks are well-defined for every pyramidal disk packing.

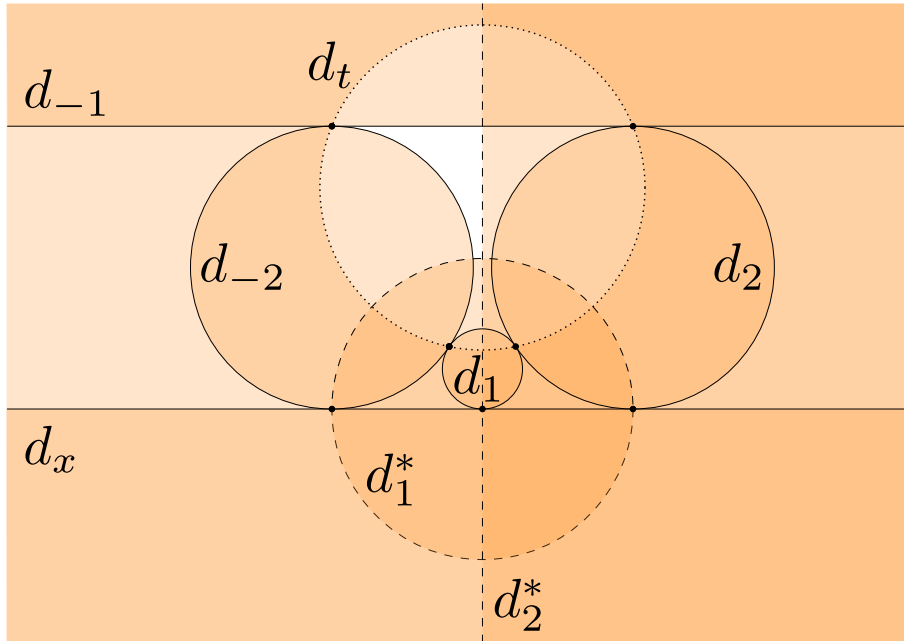


FIGURE 11. A pyramidal disk system of a standard $\mathcal{S}_x^{-1} \mathcal{D}_{\boxtimes}$ with the center of d_1 contained in the y -axis. The boundaries of the mirror disks in dashed and for the tangency disk in dotted. The label of each disk lies on its interior.

Disks	Curvature	Center		Inversive coordinates			
d_x	0 (1)	0	-1	0	-1	1	1
d_1	κ_1	0	$-1 + \frac{1}{\kappa_1}$	0	$1 - \kappa_1$	-1	$-1 + \kappa_1$
d_2	1	$\frac{2}{\sqrt{\kappa_1}}$	0	$\frac{2}{\sqrt{\kappa_1}}$	0	$\frac{2}{\kappa_1} - 1$	$\frac{2}{\kappa_1}$
d_{-1}	0 (1)	0	1	0	1	1	1
d_{-2}	1	$-\frac{2}{\sqrt{\kappa_1}}$	0	$-2 - \frac{2}{\sqrt{\kappa_1}}$	0	$\frac{2}{\kappa_1} - 1$	$\frac{2}{\kappa_1}$
d_1^*	$\frac{\sqrt{\kappa_1}}{2}$	0	-1	0	$-\frac{\sqrt{\kappa_1}}{2}$	$-\frac{1}{\sqrt{\kappa_1}}$	$-\frac{2 - \kappa_1}{2\sqrt{\kappa_1}}$
d_2^*	0 (0)	1	0	1	0	0	0
d_t	$-\frac{\kappa_1}{\sqrt{\kappa_1^2 + 4}}$	0	$\frac{2}{\kappa_1}$	0	$-\frac{2}{\sqrt{\kappa_1^2 + 4}}$	$\frac{\kappa_1}{\sqrt{\kappa_1^2 + 4}}$	0

TABLE 1. Curvature, center and inversive coordinates of the disks of the pyramidal disk system of the Figure 11 in terms of the curvature of d_1 . When a disk is a half-space the algebraic distance is given in brackets and the coordinates of the center are the coordinates of the normal vector.

Given the inversive coordinates of Table 1 we may compute the inversive products of the disks of a pyramidal disk system for each equivalence class of $\mathcal{M}^2(\boxtimes)$ in terms of the standard curvatures.

Lemma 2. *The following relations hold for every pyramidal disk system $(\mathcal{D}_{\boxtimes}, \mathcal{D}_{\boxtimes}^*, d_t)$ and for every $i = 1, 2$:*

- (a) $\langle d_i, d_{-i} \rangle = -1 - 2\kappa_i = -1 - \frac{8}{\kappa_j}$ with $i \neq j$.
- (b) $\kappa_i = \kappa_{-i}$.
- (c) $\kappa_1 \kappa_2 = 4$.
- (d) $-7 < \langle d_i, d_{-i} \rangle < -1$.
- (e) $(1 - \langle d_1, d_{-1} \rangle)(1 - \langle d_2, d_{-2} \rangle) = 16$.
- (f) $\partial d_t \subset d_1 \cup d_2 \cup d_{-1} \cup d_{-2}$.
- (g) d_1^*, d_2^* and d_t are mutually orthogonal.
- (h) $\sigma_{d_i^*}(d_j) = \begin{cases} d_{-j} & \text{if } i = |j| \\ d_j & \text{otherwise} \end{cases}$ for every $j \in \{1, 2, -1, -2, t\}$.

Proof. The relations can be obtained by simple calculations (combining equation (9) and the inversive coordinates given in Table 1). \square

The equalities (a), (b) and (c) tell us that a pyramidal disk packing has essentially two different standard curvatures κ_1 and κ_2 which are inversely proportional and the minimal standard curvature must verify $1 < \kappa \leq 2$. We define the *closest disjoint pair* of \mathcal{D}_{\boxtimes} the disjoint pair $\{d_i, d_{-i}\}$ satisfying $\kappa = \kappa_i$, $i = 1$ or 2 . The other disjoint pair will be called the *furthest disjoint pair*. In the following we use the indices $\{d_c, d_{-c}\}$ and $\{d_f, d_{-f}\}$ with $\{c, f\} = \{1, 2\}$ and $c \neq f$ to denote the *closest* and the *furthest* disjoint pair of \mathcal{D}_{\boxtimes} . By convention, we take $c = 1$ and $f = 2$ when $\kappa_1 = \kappa_2$.

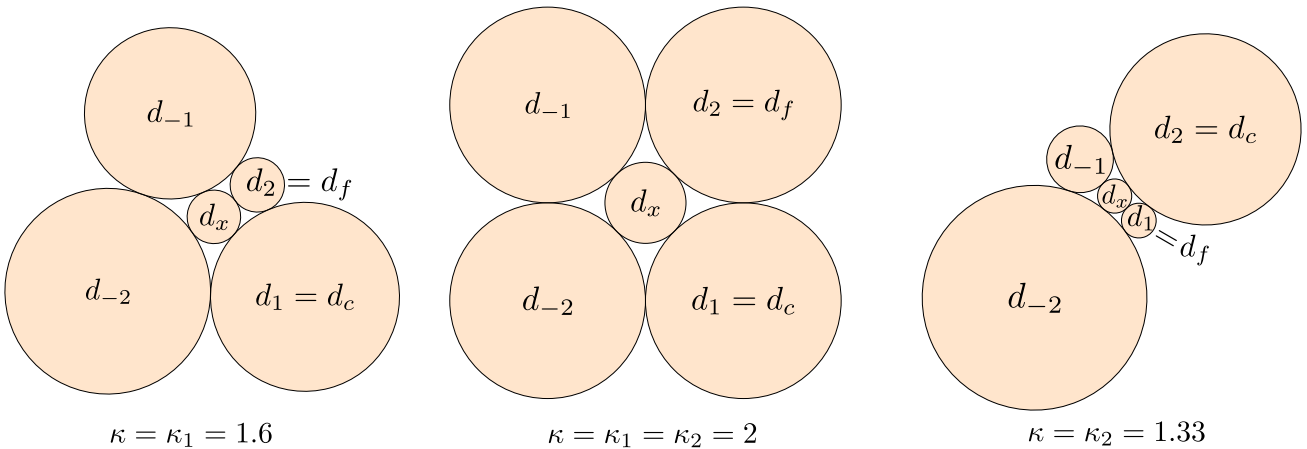


FIGURE 12. The closest and the furthest disjoint pairs in three different cases.

3.2. The crossing ball system. The main strategy for the proof of our main result is to construct a local ball packing around each crossing of the give diagram. We then stick together the local ball packings of two consecutive crossings. These local packings must take into account which piece of the curve goes over/under the other at each crossing of the link diagram. To this end, we may introduce *crossing ball systems* which are made from the blowing-up of a pyramidal disk system. There will be an over/under choice which is determined by a signed parameter $\epsilon \in \{+, -\}$.

Remark 3. *The blowing up operation preserves the inversive product.*

A *pyramidal ball packing* $\mathcal{B}_{\boxtimes} = \{b_x, b_1, b_2, b_{-1}, b_{-2}\}$ is a ball packing obtained by blowing-up a pyramidal disk packing. We define equivalently the closest and furthest disjoint pairs as in the disks case. Let $(\mathcal{D}_{\boxtimes}, \mathcal{D}_{\boxtimes}^*, d_t)$ be a pyramidal disk system. We define for every $\epsilon \in \{+, -\}$, a *crossing ball system* $(\mathcal{B}_{\boxtimes}, \mathcal{B}_{\boxtimes}^*, b_t, \mathcal{B}_{\lambda}^{\epsilon})$ as the collection of balls formed by:

- The *pyramid ball packing* \mathcal{B}_{\boxtimes} : the blowing-up of \mathcal{D}_{\boxtimes} .
- The *mirror balls* $\mathcal{B}_{\boxtimes}^* = \{b_1^*, b_2^*\}$: the blowing-up of the mirror disks $\mathcal{D}_{\boxtimes}^* = \{d_1^*, d_2^*\}$.
- The *tangency ball* b_t : the blowing-up of the tangency disk d_t .
- The *bridge balls* $\mathcal{B}_{\lambda}^{\epsilon} = \{b_3^{\epsilon}, b_{-3}^{\epsilon}\}$: the pair of balls satisfying the following conditions:
 - b_3^{ϵ} is externally tangent to b_c, b_f, b_x , internally tangent to b_c^* and contained in the half-space $\{\epsilon z \geq 0\}$, where $\{b_c, b_{-c}\}$ and $\{b_f, b_{-f}\}$ denotes the closest and the furthest pair of \mathcal{B}_{\boxtimes} .
 - b_{-3}^{ϵ} is the ball obtained by the inversion of b_3^{ϵ} on the mirror ball b_c^* .

We also define the *crossing region* \mathcal{R} of a crossing ball system as

$$\mathcal{R} = \left(\bigcap_{b \in \mathcal{B}_{\boxtimes}} -b \right) \cap b_t$$

Examples of crossing ball systems (highlighting the bridge balls) together with the corresponding crossing region are illustrated in Figure 13.

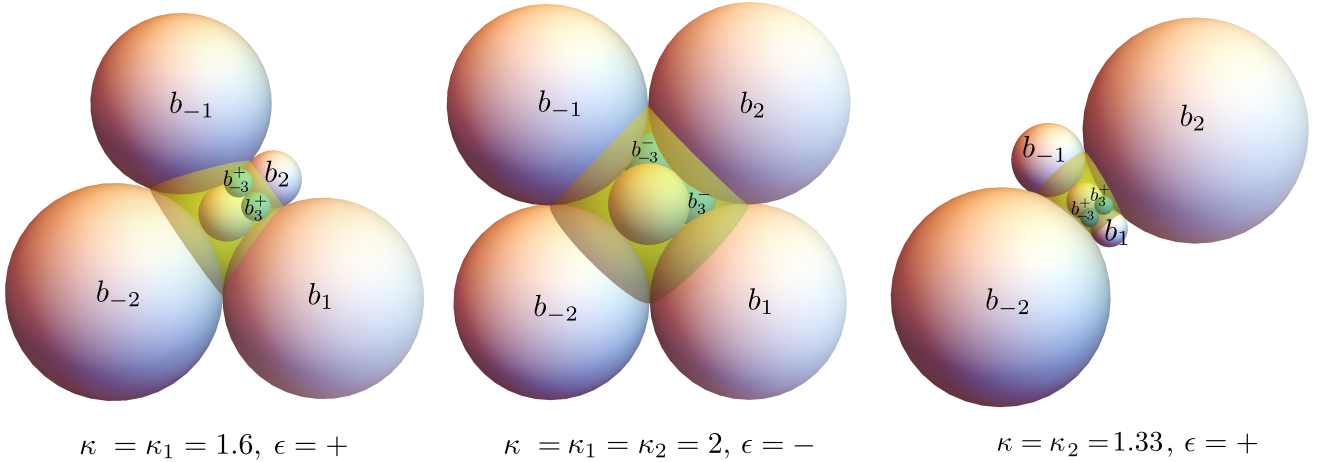


FIGURE 13. The pyramidal ball packing, bridge balls (blue) and crossing region (yellow) of three crossing ball systems seen from above.

Lemma 3. *Let $(\mathcal{B}_{\boxtimes}, \mathcal{B}_{\boxtimes}^*, b_t, \mathcal{B}_{\wedge}^{\epsilon})$ be a crossing ball system. The bridge balls b_3^{ϵ} and b_{-3}^{ϵ} are well-defined for every $\epsilon \in \{+, -\}$. Moreover, they are externally tangent and both are contained in the crossing region \mathcal{R} .*

Proof. Consider the collection of balls

$$\mathcal{B} = \{b_x, b_c, b_f, b_c^*, b_{\epsilon z}\}$$

where $\{b_c, b_{-c}\}$ and $\{b_f, b_{-f}\}$ are the closest and the furthest disjoint pair of \mathcal{B}_{\boxtimes} and $b_{\epsilon z}$ is the half-space $\{\epsilon z \geq 0\}$. Since the inversive product is preserved by the blowing-up operation, we can compute the Gramian of \mathcal{B} by using the inversive coordinates given in the Table 1 in terms of the minimal standard curvature.

$$\text{Gram}(\mathcal{B}) = \begin{pmatrix} 1 & -1 & -1 & 0 & 0 \\ -1 & 1 & -1 & \sqrt{\kappa} & 0 \\ -1 & -1 & 1 & 0 & 0 \\ 0 & \sqrt{\kappa} & 0 & 1 & 0 \\ 0 & 0 & 0 & 0 & 1 \end{pmatrix} \quad \text{and} \quad \text{Gram}(\mathcal{B})^{-1} = \frac{1}{2} \begin{pmatrix} \frac{\kappa}{2} & -1 & \frac{\kappa}{2} - 1 & \sqrt{\kappa} & 0 \\ -1 & 0 & -1 & 0 & 0 \\ \frac{\kappa}{2} - 1 & -1 & \frac{\kappa}{2} & \sqrt{\kappa} & 0 \\ \sqrt{\kappa} & 0 & \sqrt{\kappa} & 2 & 0 \\ 0 & 0 & 0 & 0 & 2 \end{pmatrix}$$

Since $\det(\text{Gram}(\mathcal{B})) = 4 \neq 0$ the Lorentzian vectors of \mathcal{B} form a basis of $\mathbb{L}^{4,1}$. In order to show that the bridge balls are well-defined we compute the polyspherical coordinates of b_3^{ϵ} respect to \mathcal{B} using the definition of b_3^{ϵ} and equation (7):

$$(12) \quad P_{\mathcal{B}}(b_3^{\epsilon}) = \begin{pmatrix} -1 \\ -1 \\ -1 \\ 1 \\ \lambda_{z,3} \end{pmatrix} \quad \text{with} \quad \lambda_{z,3} \geq 1.$$

By using equation (5) we can normalize to get $\lambda_{z,3} = \sqrt{3 + 2\sqrt{\kappa} - \kappa}$. It can be checked that $\lambda_{z,3} > 1$ for every $1 < \kappa \leq 2$. The latter implies the existence and the uniqueness of b_3^{ϵ} and hence for $b_{-3}^{\epsilon} := \sigma_{b_c^*}(b_3^{\epsilon})$ for every pyramidal ball packing. Moreover,

$$\begin{aligned} \langle b_3^{\epsilon}, b_{-3}^{\epsilon} \rangle &= \langle b_3^{\epsilon}, \sigma_{b_c^*}(b_3^{\epsilon}) \rangle \\ &= \langle b_3^{\epsilon}, b_3^{\epsilon} - 2\langle b_3^{\epsilon}, b_c^* \rangle b_c^* \rangle && \text{by (10)} \\ &= 1 - 2\langle b_3^{\epsilon}, b_c^* \rangle^2 \\ &= -1 \end{aligned}$$

so b_3^{ϵ} and b_{-3}^{ϵ} are externally tangent.

A ball b' is contained in the crossing region of the crossing ball system $(\mathcal{B}_{\boxtimes}, \mathcal{B}_{\boxtimes}^*, b_t, \mathcal{B}_{\wedge}^{\epsilon})$ if and only if

$$(13) \quad \langle b, b' \rangle \leq -1 \quad \text{for every } b \in \{b_x, b_c, b_f, b_{-c}, b_{-f}\} \quad \text{and} \quad \langle b_t, b' \rangle \geq 1$$

By combining the invariance of the inversive product under inversions, the angle between the mirrors and the other balls given in Lemma 2 (h) and the tangency conditions in the definition of b_3^{ϵ} we obtain

$$\begin{aligned} \langle b_x, b_{-3}^{\epsilon} \rangle &= \langle \sigma_{b_c^*}(b_x), \sigma_{b_c^*}(b_{-3}^{\epsilon}) \rangle = \langle b_x, b_3^{\epsilon} \rangle = -1, \\ \langle b_{-c}, b_{-3}^{\epsilon} \rangle &= \langle \sigma_{b_c^*}(b_{-c}), \sigma_{b_c^*}(b_{-3}^{\epsilon}) \rangle = \langle b_{-c}, b_3^{\epsilon} \rangle = -1 \quad \text{and} \\ \langle b_f, b_{-3}^{\epsilon} \rangle &= \langle \sigma_{b_c^*}(b_f), \sigma_{b_c^*}(b_{-3}^{\epsilon}) \rangle = \langle b_f, b_3^{\epsilon} \rangle = -1. \end{aligned}$$

For the rest of inversive products we use Lemma 2 (h), equation (5) and the inversive coordinates of Table 1 :

$$\begin{aligned} \langle b_c, b_{-3}^{\epsilon} \rangle &= \langle \sigma_{b_c^*}(b_c), \sigma_{b_c^*}(b_{-3}^{\epsilon}) \rangle = \langle b_{-c}, b_3^{\epsilon} \rangle \\ &= P_{\mathcal{B}}(b_{-c})^T \text{Gram}(\mathcal{B})^{-1} P_{\mathcal{B}}(b_3^{\epsilon}) \\ &= (-1 \quad -2\kappa + 1 \quad -1 \quad -\sqrt{\kappa} \quad 0) \text{Gram}(\mathcal{B})^{-1} \begin{pmatrix} -1 \\ -1 \\ -1 \\ 1 \\ \sqrt{3 + 2\sqrt{\kappa} - \kappa} \end{pmatrix} \\ &= -1 - 2\sqrt{\kappa} < -1 \quad \text{for } 1 < \kappa \leq 2. \end{aligned}$$

By the same procedure we obtain:

$$\begin{aligned} \langle b_{-f}, b_{-3}^{\epsilon} \rangle &= \langle \sigma_{b_c^*}(b_{-f}), \sigma_{b_c^*}(b_{-3}^{\epsilon}) \rangle = \langle b_{-f}, b_3^{\epsilon} \rangle = 3 - \frac{4}{\sqrt{\kappa}} - \frac{8}{\kappa} < -1 && \text{for } 1 < \kappa \leq 2 \quad \text{and} \\ \langle b_t, b_{-3}^{\epsilon} \rangle &= \langle \sigma_{b_c^*}(b_t), \sigma_{b_c^*}(b_{-3}^{\epsilon}) \rangle = \langle b_t, b_3^{\epsilon} \rangle = \frac{2 + 2\sqrt{\kappa} - \kappa}{\sqrt{4 + \kappa^2}} \geq 1 && \text{for } 1 < \kappa \leq 2. \end{aligned}$$

□

4. THE PROOF OF THE MAIN THEOREM.

4.1. From links to disk packable graphs. The *shadow* $\mathfrak{S}(\mathcal{L})$ of a link diagram \mathcal{L} is the planar embedding of the 4-regular graph where the vertices are the crossings and the edges are the arcs between two crossings. The *medial* of a planar graph G , denoted $\text{med}(G)$, is constructed by placing one vertex on each edge of G and joining two vertices if the corresponding edges are consecutive on a face of G . We notice that medial graphs are also 4-regular planar graphs not necessarily simple, i.e., they may contain loops and multiple edges. The *simplified medial graph* of G , denoted $\underline{\text{med}}(G)$, is the planar graph obtained from $\text{med}(G)$ by deleting loops and multiple edges. We define the *pyramidal patchwork* of a link diagram \mathcal{L} the planar graph given by the simultaneous drawing of $\mathfrak{S}(\mathcal{L}) \cup \underline{\text{med}}(\mathfrak{S}(\mathcal{L}))$ and we denote this graph $\mathfrak{X}(\mathcal{L}) = (V_{\otimes}, E_{\otimes})$. The set of vertices can be divided in two sets $V_{\otimes} = V_{\times} \cup V_{\circ}$ where V_{\times} is the set of vertices of $\mathfrak{S}(\mathcal{L})$ and V_{\circ} is the set of vertices of $\underline{\text{med}}(\mathfrak{S}(\mathcal{L}))$. We call the vertices of V_{\times} the *crossing vertices*.

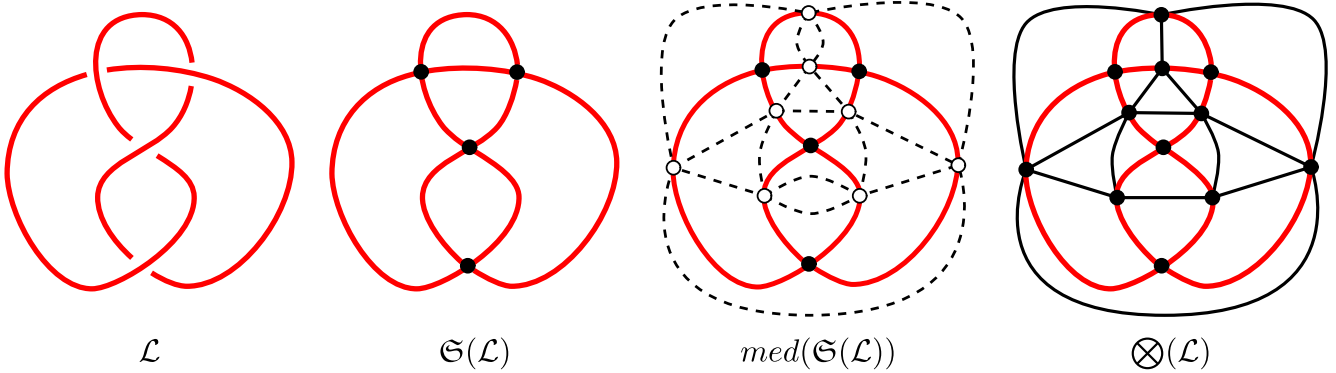


FIGURE 14. (From left to right) A diagram of the Figure 8 knot, the shadow with the crossing vertices, the medial of the shadow (dashed and white vertices) and the pyramidal patchwork.

We notice that pyramidal patchworks are simple planar graphs which are made out of the union of pyramidal graphs. If $cr(\mathcal{L})$ is the number of crossings of \mathcal{L} then we have

$$(14) \quad |V_{\otimes}| = |V_{\times}| + |V_{\circ}| = cr(\mathcal{L}) + \frac{1}{2}(4cr(\mathcal{L})) = 3cr(\mathcal{L})$$

We now have all the ingredients to proceed with the proof of Theorem 1.

4.2. Proof of theorem 1. Let \mathcal{L} be a minimal crossing diagram of L . By the KAT theorem, there is a disk packing $\mathcal{D}_{\mathfrak{X}(\mathcal{L})}$ with tangency graph $\mathfrak{X}(\mathcal{L}) = (V_{\times} \cup V_{\circ}, E_{\otimes})$. Let $\mathcal{B}_{\mathfrak{X}(\mathcal{L})}$ be the blowing-up $\mathcal{D}_{\mathfrak{X}(\mathcal{L})}$. For every crossing vertex $x \in V_{\times}$, $\mathcal{D}_{\mathfrak{X}(\mathcal{L})}$ admits a pyramidal disk system $(\mathcal{D}_{\boxtimes}(x), \mathcal{D}_{\boxtimes}^*(x), d_t(x))$ and therefore $\mathcal{B}_{\mathfrak{X}(\mathcal{L})}$ admits a crossing ball system $(\mathcal{B}_{\boxtimes}(x), \mathcal{B}_{\boxtimes}^*(x), b_t(x), \mathcal{B}_{\lambda^x}(x))$ with crossing region $\mathcal{R}(x)$. Notice that

$$\mathcal{D}_{\mathfrak{X}(\mathcal{L})} = \bigcup_{x \in V_{\times}} \mathcal{D}_{\boxtimes}(x) \quad \text{and} \quad \mathcal{B}_{\mathfrak{X}(\mathcal{L})} = \bigcup_{x \in V_{\times}} \mathcal{B}_{\boxtimes}(x).$$

We choose ϵ such that the thread of the chain made by the balls $(b_c, b_3^\epsilon(x), b_{-3}^\epsilon(x), b_{-c})$ is over/under the thread of the chain (b_f, b_x, b_{-f}) according to the diagram \mathcal{L} . We define

$$\mathcal{B}_{\Lambda(\mathcal{L})} = \bigcup_{x \in V_{\times}} \mathcal{B}_{\lambda^x}(x)$$

as the collection of all the bridge balls with the appropriate signs with respect to \mathcal{L} for each crossing vertex. Let $\mathcal{B}_{\mathcal{L}}$ be the ball collection $\mathcal{B}_{\mathfrak{X}(\mathcal{L})} \cup \mathcal{B}_{\Lambda(\mathcal{L})}$. If $\mathcal{B}_{\mathcal{L}}$ were a packing then it would contain a polygonal link in its carrier isotopic to L (by construction). Moreover, the number of balls $|\mathcal{B}_{\mathcal{L}}| = |\mathcal{B}_{\mathfrak{X}(\mathcal{L})}| + |\mathcal{B}_{\Lambda(\mathcal{L})}| = 3cr(\mathcal{L}) + 2cr(\mathcal{L}) = 5cr(\mathcal{L})$ since \mathcal{L} is a minimal crossing diagram.

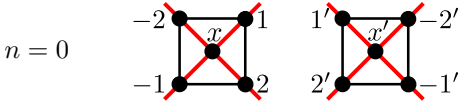
We need thus to show that $\mathcal{B}_{\mathcal{L}}$ is a packing. To this end, it is enough to show the following three claims:

- (1) $\mathcal{B}_{\mathfrak{X}(\mathcal{L})}$ is a packing.
- (2) $\mathcal{B}_{\Lambda(\mathcal{L})}$ is a packing.
- (3) Every ball of $\mathcal{B}_{\Lambda(\mathcal{L})}$ is internally disjoint to every ball of $\mathcal{B}_{\mathfrak{X}(\mathcal{L})}$.

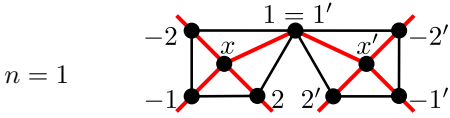
Claim (1)] It is trivial since the blowing-up operation preserves the inversive product.

Claim (3)] Let x be a crossing vertex with crossing system $(\mathcal{D}_{\boxtimes}(x), \mathcal{D}_{\boxtimes}^*(x), d_t(x))$. Since $\mathcal{D}_{\boxtimes(\mathcal{L})}$ is a packing then, as a consequence of Lemma 2 (f), any disk $d \in \mathcal{D}_{\boxtimes(\mathcal{L})} \setminus \mathcal{D}_{\boxtimes}(x)$ must be disjoint to $d_t(x)$. Therefore, the corresponding ball $b \in \mathcal{B}_{\boxtimes(\mathcal{L})} \setminus \mathcal{B}_{\boxtimes}(x)$ must be disjoint to $b_t(x)$ and thus, b is disjoint to the crossing region $\mathcal{R}(x)$ that contains the bridge balls of $\mathcal{B}_{\wedge}^e(x)$ by Lemma 3. Hence, the bridge balls of $\mathcal{B}_{\wedge}^e(x)$ are disjoint to every ball of $\mathcal{B}_{\boxtimes(\mathcal{L})} \setminus \mathcal{B}_{\boxtimes}(x)$. Moreover, Lemma 3 also ensures that the bridge balls $\mathcal{B}_{\wedge}^e(x)$ are at most tangent to the balls of $\mathcal{B}_{\boxtimes}(x)$.

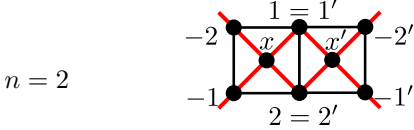
Claim (2)] We first notice that, by Lemma 3, the bridge balls of a crossing system are externally tangent. We need to show that bridge balls of different crossing systems are also internally disjoint. Let x and x' be two different crossing vertices with $\mathcal{D}_{\boxtimes}(x) = \{d_x, d_1, d_2, d_{-1}, d_{-2}\}$ and $\mathcal{D}_{\boxtimes}(x') = \{d_{x'}, d_{1'}, d_{2'}, d_{-1'}, d_{-2'}\}$. Let n be the number of disks in common of $\mathcal{D}_{\boxtimes}(x)$ and $\mathcal{D}_{\boxtimes}(x')$. We show that in each of the five cases of $n = 0, 1, 2, 3, 4$ the crossing regions $\mathcal{R}(x)$ and $\mathcal{R}(x')$ are internally disjoint (implying that the bridge balls of $\mathcal{B}_{\wedge}^e(x)$ and $\mathcal{B}_{\wedge}^e(x')$ are at the most tangent). If needed we may relabel $\mathcal{D}_{\boxtimes}(x')$ in order to work with the same labelling of the graphs showed at the left in each case.



Since $\mathcal{D}_{\boxtimes(\mathcal{L})}$ is a packing then, by Lemma 2 (f), the boundaries $\partial d_t(x)$ and $\partial d_t(x')$ are disjoint. Therefore, $d_t(x)$ and $d_t(x')$ are disjoint as well as $b_t(x)$ and $b_t(x')$. Hence, $\mathcal{R}(x) \cap \mathcal{R}(x') = \emptyset$.



The (possible empty) region $d_t(x) \cap d_t(x')$ must be contained in d_1 so $b_t(x) \cap b_t(x')$ is contained in b_1 . As a consequence, $int(\mathcal{R}(x)) \cap int(\mathcal{R}(x')) = \emptyset$.



We can apply a standard transformation to get a standard disk packing $\mathcal{S}_2^1(\mathcal{D}_{\boxtimes}(x) \cup \mathcal{D}_{\boxtimes}(x'))$ where the disks $d_1, d_2, d_t(x)$ and $d_t(x')$ become half-spaces as in Figure 15.

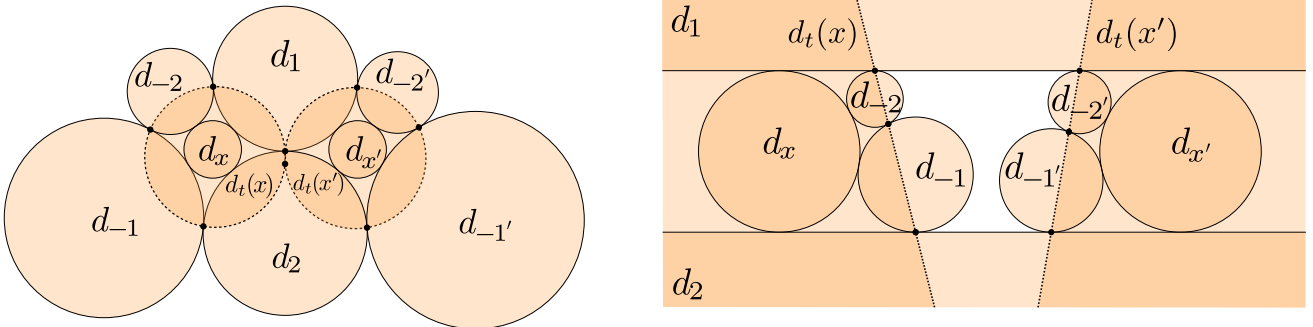
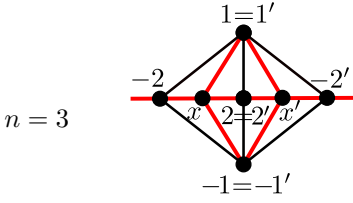


FIGURE 15. Left, $\mathcal{D}_{\boxtimes}(x) \cup \mathcal{D}_{\boxtimes}(x')$ with two common disks, together with their tangency disks. Right, $\mathcal{S}_2^1(\mathcal{D}_{\boxtimes}(x) \cup \mathcal{D}_{\boxtimes}(x'))$.

The lines $\partial d_t(x)$ and $\partial d_t(x')$ in $\mathcal{S}_2^1(\mathcal{D}_{\boxtimes}(x) \cup \mathcal{D}_{\boxtimes}(x'))$ either intersect in a point lying in $d_1 \cup d_2$ or they are parallel implying, in both cases, that the region $d_t(x) \cap d_t(x')$ is contained in $d_1 \cup d_2$. Therefore, $b_t(x) \cap b_t(x')$ is contained in $b_1 \cup b_2$ and thus $int(\mathcal{R}(x)) \cap int(\mathcal{R}(x')) = \emptyset$.



The boundaries of $d_t(x)$ and $d_t(x')$ intersect at the tangency points of $d_1 \cap d_2$ and $d_{-1} \cap d_2$, see Figure 16. Therefore $d_t \cap d_t'$ is contained in d_2 which implies that $b_t \cap b_t'$ is contained in b_2 and hence $int(\mathcal{R}) \cap int(\mathcal{R}') = \emptyset$.

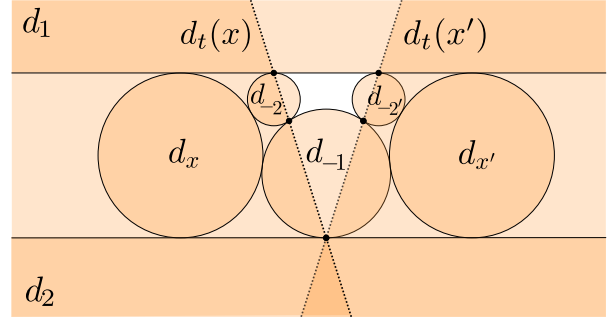
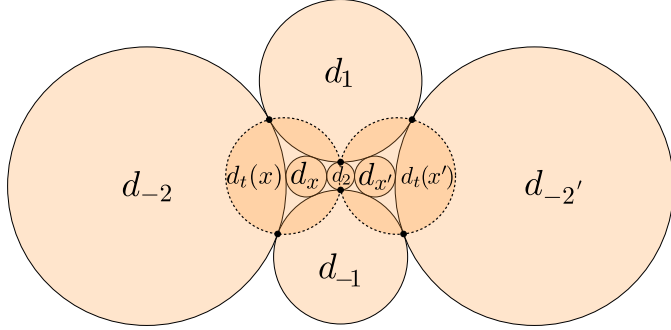
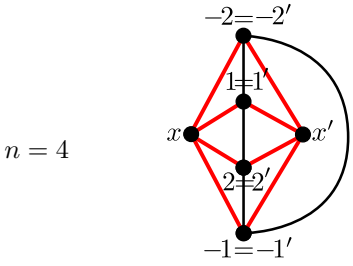


FIGURE 16. (Left) $\mathcal{D}_{\boxtimes}(x) \cup \mathcal{D}_{\boxtimes}(x')$ with three common disks, together with their tangency disks. (Right) $\mathcal{S}_2^1(\mathcal{D}_{\boxtimes}(x) \cup \mathcal{D}_{\boxtimes}(x'))$.



In this case, the tangency graph of $\mathcal{D}_{\boxtimes}(x) \cup \mathcal{D}_{\boxtimes}(x')$ is isomorphic to the octahedral graph by taking $x' = 3$ and $x = -3$. We have that $d_t(x) = -d_t(x')$ and so $b_t(x)$ and $b_t(x')$ are externally tangent implying that $int(\mathcal{R}(x)) \cap int(\mathcal{R}(x')) = \emptyset$.

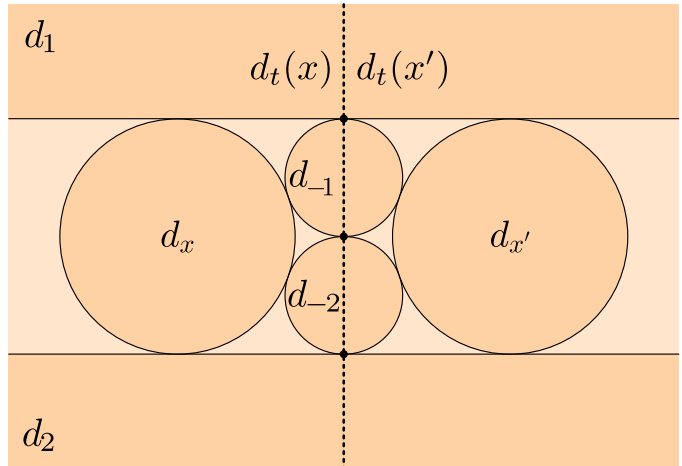
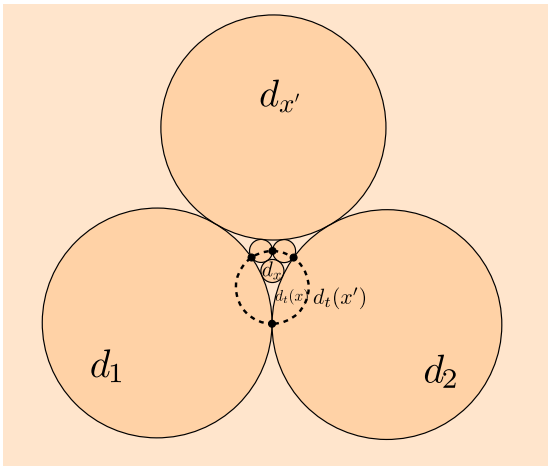


FIGURE 17. (Left) $\mathcal{D}_{\boxtimes}(x) \cup \mathcal{D}_{\boxtimes}(x')$ with four common disks which leads to the octahedral disk packing. (Right) $\mathcal{S}_2^1(\mathcal{D}_{\boxtimes}(x) \cup \mathcal{D}_{\boxtimes}(x'))$.

□

5. THE NECKLACE ALGORITHM

In this section we present an algorithm arised from the constructive proof of our main result. Our necklaces figures are based on this algorithm.

The balls are given in inversive coordinates. Instead of computing the bridge balls by using the basis with the mirror ball b_c^* (as done in the proof of Lemma 3), we use the basis $\mathcal{B} = \{b_x, b_c, b_f, b_{-c}, b_{\epsilon z}\}$ which avoids the computation of b_c^* . To this end, we need the inversive products $\lambda_{-c,3} := \langle b_{-c}, b_3^\epsilon \rangle = \langle b_c, b_{-3}^\epsilon \rangle$ and $\lambda_{z,3} := \langle b_{\epsilon z}, b_3^\epsilon \rangle = \langle b_{\epsilon z}, b_{-3}^\epsilon \rangle$. These values are given in the proof of Lemma 3 in terms of the minimal standard curvature by $\lambda_{-c,3} = -1 - 2\sqrt{\kappa}$ and $\lambda_{z,3} = \sqrt{3 + 2\kappa - \kappa}$. The minimal standard curvature can be computed by using Lemma 2 (a) obtaining $\kappa = \frac{1-\lambda_{c,-c}}{2} = \frac{8}{1-\lambda_{f,-f}}$ where $\lambda_{c,-c} := \langle b_c, b_{-c} \rangle$ and $\lambda_{f,-f} := \langle b_f, b_{-f} \rangle$. In order to obtain a disk packing from the tangency graph we use the well-known algorithm of Collins and Stephenson given in [9] where the radius of the outer disks and the visual precision can be chosen. In all our examples we set the outer radii to be equal to 1 and precision 10^{-4} .

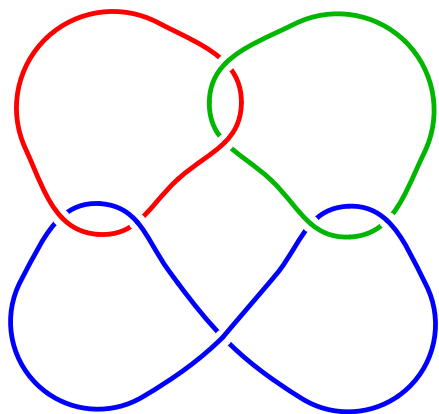
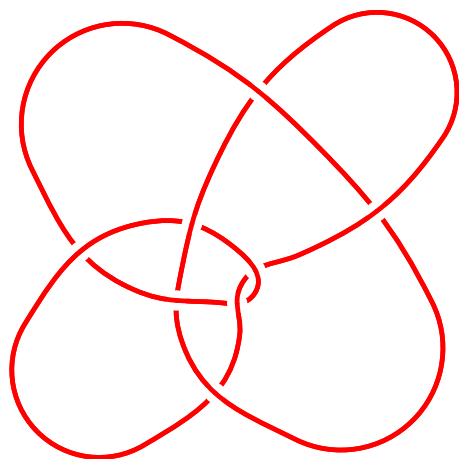
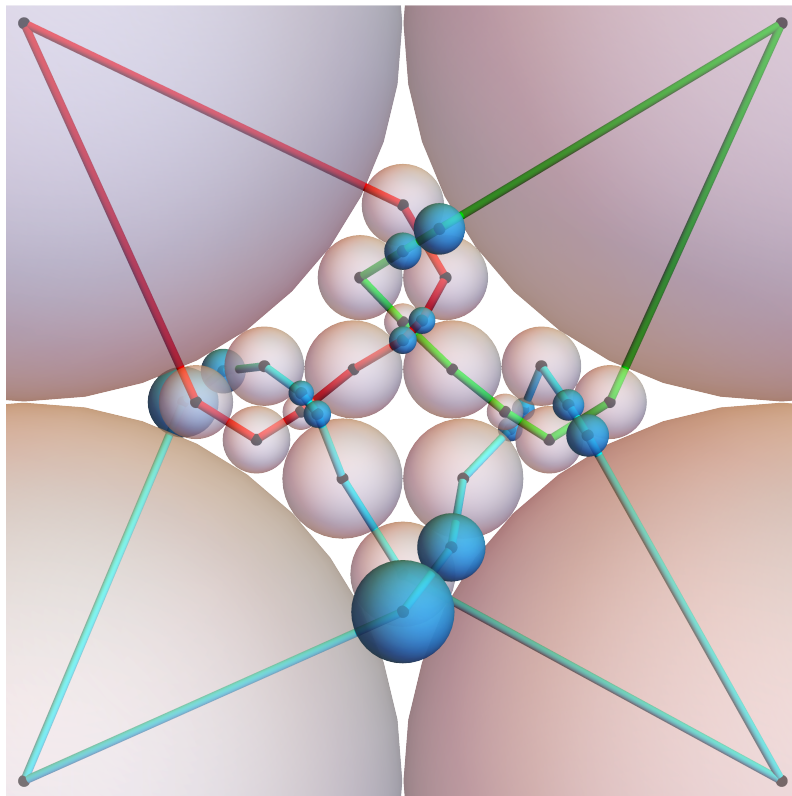
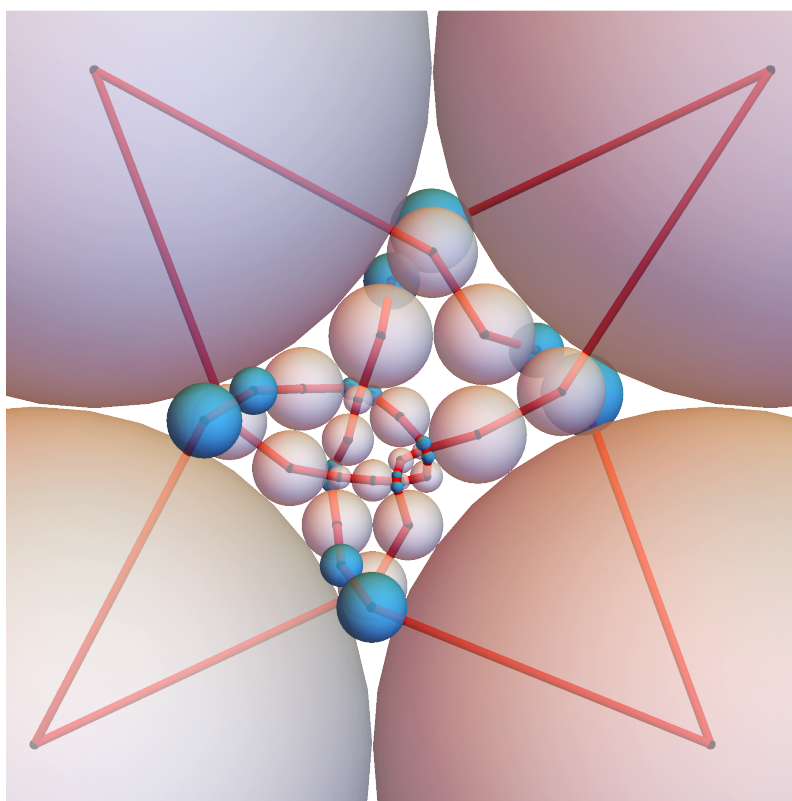
TABLE 2. Necklace algorithm

Input: A link diagram \mathcal{L} with n crossings of a link L .

Output: A necklace representation $\mathcal{B}_{\mathcal{L}}$ of the link L with $5n$ balls.

Algorithm:

1. Construct the pyramidal patchwork $\otimes(\mathcal{L}) = (V_{\times} \cup V_{\circ}, E_{\otimes})$
2. Construct a disk packing $\mathcal{D}_{\otimes(\mathcal{L})}$ of tangency graph $\otimes(\mathcal{L})$
3. Construct a ball packing $\mathcal{B}_{\otimes(\mathcal{L})}$ obtained by blowing-up $\mathcal{D}_{\otimes(\mathcal{L})}$
4. Set $\mathcal{B}_{\wedge(\mathcal{L})} = \{\}$, $Q = \text{diag}(1, 1, 1, 1, -1)$, $b_z = (0 \ 0 \ 1 \ 0 \ 0)^T$
5. **For** $x \in V_{\times}$ **do:**
 - (a) Give to $\mathcal{B}_{\boxtimes}(x)$ a pyramid labeling $\mathcal{B}_{\boxtimes}(x) = \{b_x, b_1, b_2, b_{-1}, b_{-2}\}$
 - (b) Compute the inversive product $\lambda = b_1^T Q b_{-1}$
 - (c) **If** $\lambda \geq -3$ **then:**
 - i. $B = (b_x | b_1 | b_2 | b_{-1} | b_z)$, $\kappa = \frac{1-\lambda}{2}$
 - (d) **else:**
 - i. $B = (b_x | b_2 | b_1 | b_{-2} | b_z)$, $\kappa = \frac{8}{1-\lambda}$
 - (e) $\lambda_{-c,3} = -1 - 2\sqrt{\kappa}$, $\lambda_{z,3} = \sqrt{3 + 2\kappa - \kappa}$
 - (f) $b_3(x) = ((-1 \ -1 \ -1 \ \lambda_{-c,3} \ \lambda_{z,3}) B^{-1} Q)^T$
 - (g) $b_{-3}(x) = ((-1 \ \lambda_{-c,3} - 1 \ -1 \ \lambda_{z,3}) B^{-1} Q)^T$
 - (h) **If** the thread made by the bridge balls is under-crossing in \mathcal{L} **then:**
 - i. $b_3(x) \leftarrow \text{diag}(1 \ 1 \ -1 \ 1 \ 1) b_3(x)$
 - ii. $b_{-3}(x) \leftarrow \text{diag}(1 \ 1 \ -1 \ 1 \ 1) b_{-3}(x)$
 - (i) $\mathcal{B}_{\wedge(\mathcal{L})} \leftarrow \mathcal{B}_{\wedge(\mathcal{L})} \cup \{b_3(x), b_{-3}(x)\}$
6. $\mathcal{B}_{\mathcal{L}} = \mathcal{B}_{\otimes(\mathcal{L})} \cup \mathcal{B}_{\wedge(\mathcal{L})}$


 7_1^3

 8_{17}


Knot 4_1					Link 7_1^3					Knot 8_{17}				
Ball	x	y	z	r	Ball	x	y	z	r	Ball	x	y	z	r
1	0.	0.	0.	1.	1	0.	0.	0.	1.	1	0.	0.	0.	1.
2	0.8498	0.6641	0.	0.0785	2	0.4068	1.	-0.1882	0.0958	2	0.5168	0.958	0.2146	0.1094
3	1.	0.6603	0.	0.0718	3	0.519	1.083	-0.1184	0.0603	3	0.6549	1.0442	0.1381	0.0704
4	1.1502	0.6641	0.	0.0785	4	0.6344	1.0947	0.	0.1054	4	0.7919	1.0508	0.	0.1243
5	2.	0.	0.	1.	5	0.7338	1.0234	0.0655	0.0334	5	0.9356	1.0528	-0.0671	0.0343
6	1.	0.3213	-0.1097	0.056	6	0.7762	0.9686	0.071	0.0362	6	0.9982	1.0317	-0.0625	0.0319
7	0.9571	0.3768	-0.0593	0.0303	7	0.8407	0.7983	0.	0.1593	7	1.081	0.9676	0.	0.09
8	0.9553	0.4226	0.	0.0447	8	1.	0.5458	0.	0.1392	8	1.1502	0.8904	0.0455	0.0232
9	0.977	0.4699	0.0318	0.0163	9	2.	0.	0.	1.	9	1.164	0.8497	0.0395	0.0202
10	1.	0.495	0.0352	0.018	10	1.4814	0.9131	0.1095	0.0558	10	1.1595	0.7925	0.	0.0494
11	1.0718	0.5359	0.	0.0718	11	1.4327	0.9925	0.0815	0.0415	11	1.0879	0.7759	0.	0.0241
12	1.134	0.5796	-0.09	0.046	12	1.3656	1.0947	0.	0.1054	12	1.0007	0.7799	0.	0.0633
13	1.175	0.6784	-0.1552	0.0793	13	1.3204	0.9813	-0.0604	0.0307	13	0.902	0.7895	0.	0.0358
14	1.	1.7321	0.	1.	14	1.2858	0.9279	-0.065	0.0331	14	0.7559	0.8166	0.	0.1127
15	0.825	0.6784	0.1552	0.0793	15	1.1593	0.7983	0.	0.1593	15	0.5757	0.9527	0.	0.1132
16	0.866	0.5796	0.09	0.046	16	1.1253	0.6243	0.1733	0.0886	16	0.1772	1.9921	0.	1.
17	0.9282	0.5359	0.	0.0718	17	1.	0.4638	0.2589	0.1323	17	1.1772	1.4541	0.	0.1356
18	1.	0.4737	0.	0.0232	18	2.	2.	0.	1.	18	1.3308	1.212	0.	0.1511
19	1.0447	0.4226	0.	0.0447	19	1.0949	1.4501	0.1314	0.0671	19	1.4928	1.1678	-0.1645	0.084
20	1.	0.3342	0.	0.0544	20	1.	1.3938	0.0956	0.0489	20	1.6347	1.0364	-0.2477	0.1265
					21	0.8873	1.3285	0.	0.1127	21	2.	0.	0.	1.
					22	1.	1.211	0.	0.0501	22	1.	0.4186	0.2005	0.1025
					23	1.1302	1.0863	0.	0.1302	23	0.9104	0.5354	0.1241	0.0634
					24	1.2695	0.9745	0.	0.0485	24	0.895	0.6486	0.	0.1053
					25	1.3864	0.9006	0.	0.0898	25	0.876	0.7684	-0.0535	0.0273
					26	1.546	1.	0.	0.0982	26	0.8848	0.8205	-0.0502	0.0256
					27	0.	2.	0.	1.	27	0.9271	0.9005	0.	0.0779
					28	1.	1.5198	0.	0.1093	28	0.9571	1.0187	0.	0.044
					29	1.1127	1.3285	0.	0.1127	29	1.0243	1.2064	0.	0.1554
					30	1.0501	1.2136	0.0693	0.0354	30	1.0559	1.3765	-0.1686	0.0861
					31	1.	1.162	0.0714	0.0365	31	1.1772	1.533	-0.2525	0.1289
					32	0.8698	1.0863	0.	0.1302	32	2.1772	1.9921	0.	1.
					33	0.7305	0.9745	0.	0.0485	33	1.5588	1.0432	0.	0.1327
					34	0.6136	0.9006	0.	0.0898	34	1.3111	0.9157	0.	0.1459
					35	0.454	1.	0.	0.0982	35	1.1441	0.8682	0.	0.0278
										36	1.0843	0.8388	0.	0.0389
										37	1.0718	0.7954	0.0305	0.0156
										38	1.0717	0.7615	0.0372	0.019
										39	1.1051	0.6481	0.	0.1049
										40	1.	0.4677	0.	0.1039

REFERENCES

- H. Breu and D. Kirkpatrick, On the complexity of recognizing intersection and touching graphs of disks. In: *Brandenburg F.J. (eds) Graph Drawing, GD (Passau 1995)*, LNC, Springer, Berlin, Heidelberg, **1027** (1996), 88–98.
- K. Bezdek and S. Reid, *Contact graphs of unit sphere packings revisited*, *J. Geom.* **104**(1) (2013), 57–83.
- P. L. Bowers, Combinatorics encoding geometry: the legacy of Bill Thurston in the story of one theorem, *arXiv:2008.12357* (2020).
- D. W. Boyd, A new class of infinite sphere packings, *Pacific Journal of Mathematics* **50**(2) (1974), 283–398.
- T. E. Cecil, *Lie Sphere Geometry*, Springer-Verlag (1992).
- H. Chen, Apollonian ball packings and stacked polytopes, *Discrete Comput. Geom.* **55**(4) (2016), 80–826.
- H. Chen, Ball Packings and Lorentzian Discrete Geometry, *Freie Universitat Berlin* (2014).
- H. Chen and J.-P. Labbé, Lorentzian Coxeter Systems and Boyd-Maxwell ball packings, *Geometriae Dedicata* **174** (2015), 43–73.
- C. Collins and K. Stephenson, A circle packing algorithm, *Comput. Geom. Theor. and App.* **25** (2003), 233–256.
- Y. Diao and C. Ernst, Realizable powers of ropelengths by nontrivial knot families, *J. Geom. and Topology* **4**(2) (2004), 197–208.
- E. A. Elrifai, On sitck number of knots and links, *Chaos, Solitons and Fractals* **27** (2006), 233–236.
- G. Guettler and C. Mallows, *A generalization of Apollonian packing of circles. (2008)*
- P. Hliněný, Touching graphs of unit balls, In: *DiBattista G. (eds) Graph Drawing, GD (Rome 1997)*, LNCS, Springer, Berlin, Heidelberg, **1353** (1997), 350–358.
- P. Koebe, Kontaktprobleme der Konformen Abbildung, *Ber. Sächs. Akad. Wiss. Leipzig, Math.-Phys. Kl* **88** (1936), 141–164.
- G. Kuperberg and O. Schramm, Average kissing numbers for non-congruent sphere packings, *Math. Res. Lett.* **1**(3) (1994), 339–344.
- J. C. Lagarias, C. L. Mallows and A. R. Wilks, Beyond the Descartes circle theorem, *Amer. Math. Monthly* **109**(4) (2002), 338–361.
- H. Maehara, On Configurations of Solid Balls in 3-Space: Chromatic Numbers and Knotted Cycles, *Graphs and Combinatorics* **23** (2007), 307–320.
- H. Maehara and H. Noha, On the graph represented by a family of solid balls on a table, *Ryukyu Math. J.*, **10** (1997), 51–64.
- H. Maehara and A. Oshiro, On Soddy's hexlet and a linked 4 pair. In: *J. Akiyama et al. (eds.) Discrete and Computational Geometry. Japanese conference, JCDCG '98. Tokyo, Japan, December 9-12, 1998*, LNCS, Springer, Berlin, Heidelberg, **1763** (2000), 188–193.
- H. Maehara and A. Oshiro, On Knotted Necklaces of Pearls, *Europ. J. Combinatorics* **20** (1999), 411–420.
- K. Stephenson, *Introduction to Circle-Packing: The theory of discrete analytic functions*, Cambridge University Press (2005), pp 356.
- W. P. Thurston, *Three-Dimensional Geometry and Topology*, Princeton University Press (1997).
- J.B. Wilker, Inversive Geometry. In: Davis C., Grünbaum B., Sherk F.A. (eds) *The Geometric Vein*, Springer, New York, NY. (1981), 379–442.

UMI2924 J.-C. Yoccoz, CNRS-IMPA, BRAZIL AND IMAG, UNIV. MONTPELLIER, CNRS, MONTPELLIER, FRANCE
 Email address: jorge.ramirez-alfonsin@umontpellier.fr

IMAG, UNIV. MONTPELLIER, CNRS, MONTPELLIER, FRANCE
 Email address: ivan.rasskin@umontpellier.fr